

# NUCLEATION OF FLUX INSTABILITIES IN THIN SUPER-CONDUCTING FILMS : NANOSECOND MAGNETO-OPTIC INVESTIGATIONS

S.HERMINGHAUS, J.BONEBERG, P.BRÜLL, V.BUYOK, P.LEIDERER  
*Fakultät für Physik, Universität Konstanz, 7750 Konstanz, Germany*

## ABSTRACT

We have investigated the short time dynamics in the magnetic flux distribution of thin  $\text{YBa}_2\text{Cu}_3\text{O}_{7-x}$  films by means of time resolved magnetooptics. Local heating of the superconductor with a focussed laser pulse in a region with high shielding currents leads to an instability in the magnetic flux distribution. A pump-probe technique allowed to visualize changes in the flux distribution on a nanosecond time scale. The instability develops in two steps giving rise to additional flux penetration and to a branching of the flux front into the superconductor. An estimate of the width of the branches based on London's equations shows good agreement with the experiment.

## 1. Introduction

When a superconducting thin film is placed in a magnetic field perpendicular to it, there exists a critical field strength at which the Meissner state becomes unstable and magnetic flux penetrates into the formerly shielded region of the film. Under certain circumstances, this penetration proceeds via so-called flux jumps<sup>1-7</sup>. It has been shown that these are associated with the formation of narrow 'fingers' or strips of penetrated magnetic flux<sup>7,8</sup>. In Fig.1 this is shown by magneto-optic photography<sup>9,10</sup> of a superconducting Nb-film subject to a magnetic field of 10mT. From (a) to (c), the magnetic field is increased by a few percent. The formation of one strip (i.e., a flux jump) takes place on a time scale faster than the resolution of the video equipment, i.e., faster than 20msec. In this critical state, the superconductor is very sensitive to small perturbations. A flux jump associated with a large change in the magnetic field may then

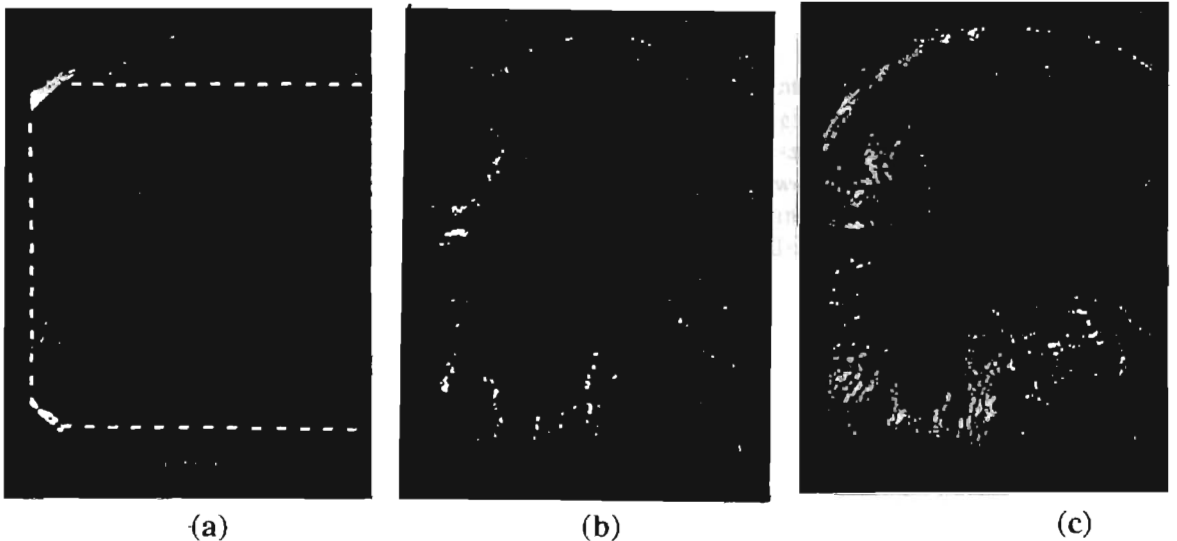


Fig.1. Flux penetration into a superconducting Nb film recorded magneto-optically. Dark: shielded regions. Bright: penetrated by magnetic field (Shubnikov phase). The bright strips are formed on a time scale which is not resolved by the video equipment used for the recording. From (a) to (c), the magnetic field is increased by a few percent, the applied field is approximately 10 mT. The dashed line in (a) indicates the sample dimensions. The film thickness is 300nm.

easily be triggered. This property is particularly interesting in view of possible applications in elementary particle detection. In order to gain insight into the physics of these flux jumps, it is desirable to determine the time scale at which they take place and the dependence of their spatial structure on external parameters.

## 2. Experiment

We have carried out magneto-optic studies of flux jumps in high- $T_C$  superconducting films since the critical fields are particularly high in these systems, giving rise to a good optical contrast in the experiment. We used epitaxial c-oriented  $\text{YBa}_2\text{Cu}_3\text{O}_{7-x}$  films with a thickness of 300nm, deposited on 1-cm<sup>2</sup>  $\text{LaAlO}_3$  substrates by laser ablation<sup>11</sup>. The measurements were carried out in an optical cryostat equipped with a superconducting magnet. The direction of the magnetic field was perpendicular to the sample plane. In order to detect the flux distribution in the sample we used a reflection magneto-optic technique, with a EuS indicator film as described earlier<sup>12</sup>. The sample was zero-field cooled and immersed in superfluid  $^4\text{He}$  at 1.8 K. As a magnetic field was applied, the evolution of the flux distribution in the sample was recorded with a video camera using a standard magneto-optic setup with a spacial resolution of 10 $\mu\text{m}$ . The field was typically increased up to a few  $10^2$  T, where flux entering from the sample edges roughly filled several ten percent of the film area, leaving a large portion of the sample in the Meissner state<sup>13</sup>. In order to perturb this state and to initiate the magnetic instability, a pulse of a frequency-doubled Nd:YAG laser ( $\lambda = 532$  nm, FWHM 7 ns, energy up to 30 mJ) was focussed onto the superconducting film from the back side through the polished substrate, as shown in fig.2. The laser focus with a diameter of 50 $\mu\text{m}$  could be positioned arbitrarily on the sample surface. At the laser energies used here the sample temperature in the focus, although not being measured directly, supposedly rose above the critical temperature of the superconductor ( $T_C = 92$  K).

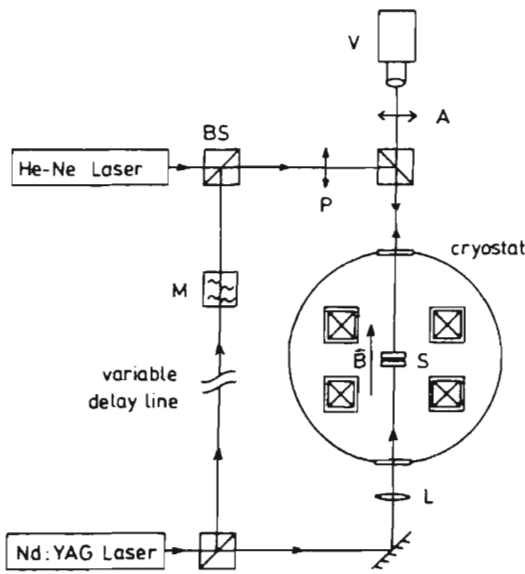


Fig.2. Experimental setup. The  $\text{YBaCuO}$  sample is covered with a glass plate carrying the magneto-optic indicator sandwich film with a distance of about 1 $\mu\text{m}$  between the superconductor and the indicator. The indicator sandwich consists of the magneto-optically active EuS layer, which is covered by aluminum to increase the reflectivity. The direction of the magnetic field,  $B$ , is perpendicular to the sample plane. BS: beam splitter; S: sample; P: polarizer; A: analyzer; V: video camera; L: lens; M: methanol cell for stimulated Raman scattering. The variable delay line serves for magneto-optic recording with nanosecond temporal resolution.

A pump-probe technique was applied to achieve the high temporal resolution necessary to determine the spreading velocity of the flux fronts. Part of the Nd:YAG beam was separated by a beam splitter, passed through a variable delay line of several tens of nsec, and frequency shifted to  $\lambda = 635$  nm<sup>10</sup>. This pulse was fed into the magneto-optic light

path to illuminate the EuS film at a well defined time delay some tens of nanoseconds after the instability had been nucleated. The comparison of the extension of the magnetic structure in this snapshot with the final flux distribution allowed to determine the spreading velocity.

### 3. Results and Discussion

In fig.3 we present examples for the steady state patterns of an  $\text{YBa}_2\text{Cu}_3\text{O}_{7-x}$  film in a constant external field,  $B_{\text{ext}} = 60\text{mT}$  in this case. Fig.3a, taken before the Nd:YAG shot, indicates some penetration of flux at the sample edges (white regions), whereas the central, dark area represents the Meissner phase. Its overall shape is a typical field penetration pattern as shown before<sup>12</sup>. It should be pointed out that due to the small film thickness comparable to the London penetration depth ( $\sim 150\text{nm}$ ) large shielding currents with current densities close to the critical current density  $j_c$  of about  $2 \times 10^7 \text{A/cm}^2$  flow even in the Meissner phase<sup>12,14</sup>. Fig.3b shows the same film after laser heating a spot approximately at the sample centre. Although somewhat difficult to discern, a rather large portion of the former Meissner region now displays an increased, nearly constant light intensity - and hence the presence of a perpendicular magnetic field - indicating that the laser pulse has nucleated a large scale redistribution of magnetic flux.

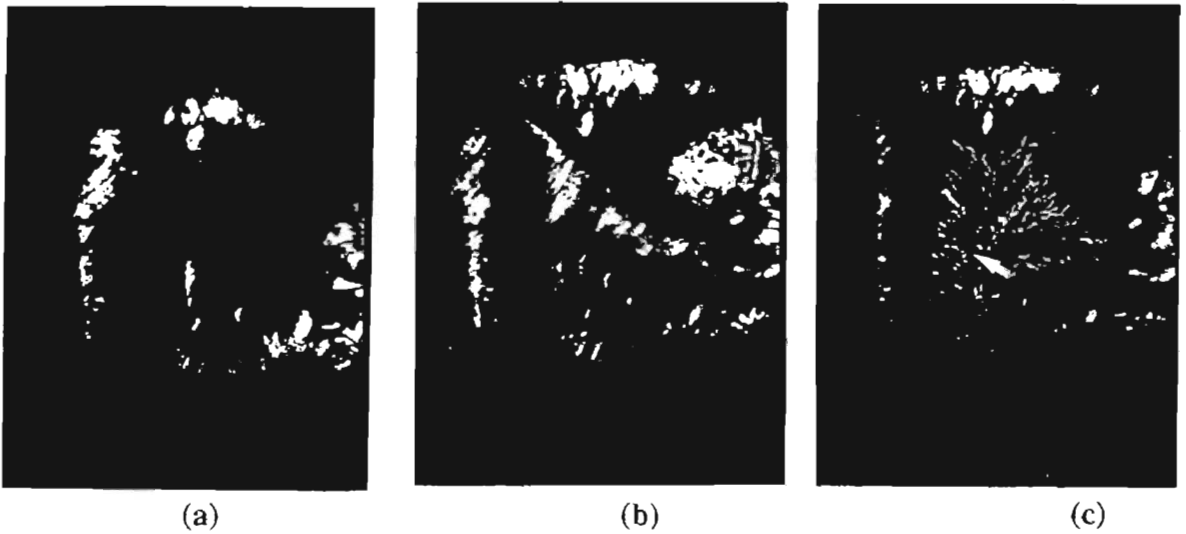


Fig.3. Laser-induced changes in the magnetic field distribution. The sample size is  $1 \times 1 \text{ cm}^2$ . (a) Flux distribution before the laser pulse ( $T = 1.8 \text{ K}$ ,  $B_{\text{ext}} = 60 \text{ mT}$ ). A major part of the sample is in the Meissner phase. (b) Change of the flux distribution after laser heating a spot in the sample center. (c) Change of the flux distribution after laser heating a spot close to a weak region (position indicated by the white arrow), where some flux had already penetrated.

Next we started again from a field distribution as depicted in Fig. 3a - after heating the sample above  $T_c$ , zero field cooling and applying  $B_{\text{ext}} = 60\text{mT}$  - but now the laser focus was adjusted near the sample edge, close to a "weak spot" where flux had already entered the film. Although the overall contour of the resulting laser-induced flux distribution, as seen in Fig.3c, is similar to the one in Fig. 3b, the fine structure is obviously completely different. Instead of the more or less spatially constant flux density in fig.3b, one now observes pronounced branchlike structures with an average spacing of  $0.3\text{mm}$  and a width of the branches of  $0.1\text{mm}$ . On closer inspection one can distinguish also in Fig.3c an area of about  $0.5 \text{ mm}$  radius around the nucleation spot with a structureless flux distribution without branches. This is a first hint that flux motion triggered by the laser pulse actually develops in two steps: i) first, a perturbation grows in the Meissner phase around the

nucleation spot in a roughly isotropic way, forming a region where flux, accumulated at some weak parts of the film before, is afterwards distributed homogeneously within the perturbed area: ii) as soon as this region makes contact with the surrounding externally applied field at some point, massive avalanche-like penetration of external flux sets in, and branches start to spread out from the rim of the homogeneous area.

More conclusive evidence for the hypothesis of such a two-step process comes from the time-resolved measurements to be discussed now. Fig.4 displays a sequence of pictures taken before (4a), 56ns after (4b) and a few seconds after (4c) the Nd:YAG pulse. Fig.4b thus represents a transient state, whereas 4a and 4c are steady distributions. A comparison of Figs. 4b and 4c shows that already after  $t=56\text{ns}$  the flux structure has nearly reached its final size. Nevertheless, some of the branches are not yet fully developed and apparently still are to grow a few tenths of a mm. A series of such recordings with variable delay times has been used to investigate the growth dynamics of the flux structures in more detail. These studies reveal that the spatially homogeneous field distributions like in Fig. 3b develop extremely fast, on a time scale which is not even accessible with our temporal resolution of 10ns. We therefore can only estimate that the speed at which the front of this phase propagates is larger than  $2 \times 10^5 \text{m/s}$ . The propagation speed of the branches, on the other hand, was small enough that it could be determined with our technique, as can be seen from fig.4. Evaluating a number of recordings<sup>15</sup> similar to the one shown in fig.4, we obtained a branch velocity of  $\langle v \rangle = (5 \pm 2) \times 10^4 \text{m/s}$ , which, for comparison, is an order of magnitude higher than the velocity of sound in  $\text{YBa}_2\text{Cu}_3\text{O}_{7-x}$ <sup>16</sup>.

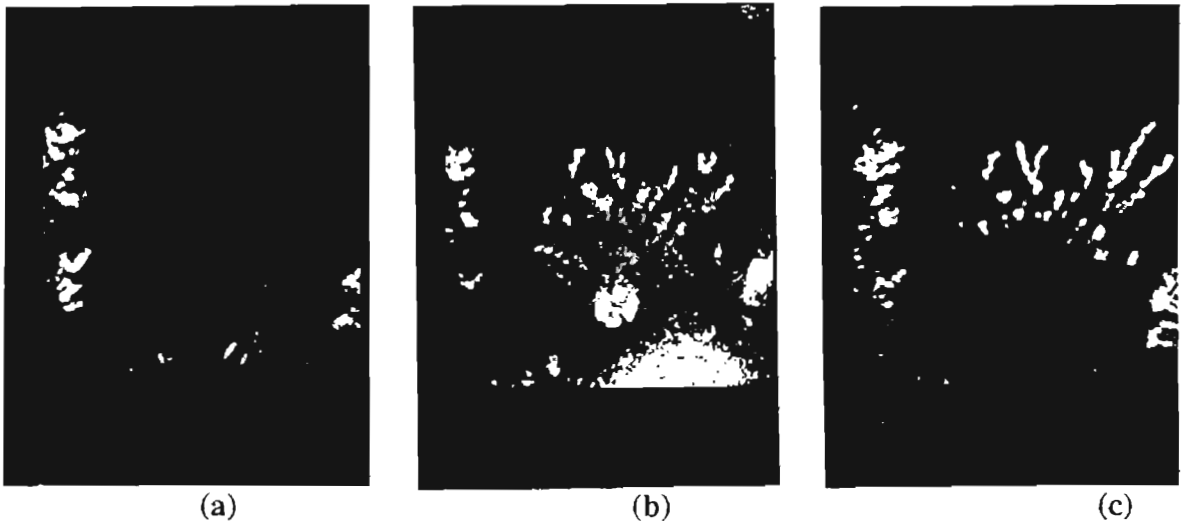


Fig.4. Time evolution of the instability in the magnetic field distribution. The frames correspond to a  $4 \times 4 \text{mm}^2$  section of the superconductor ( $T = 1.8 \text{K}$ ,  $B_{\text{ext}} = 25 \text{mT}$ ). (a) Before the laser pulse, (b) 56 nsec after the laser pulse, and (c) final flux distribution. The width of the branches is similar as in fig.3(c) ( $\approx 100 \mu\text{m}$ ).

We now turn to possible interpretations of the observed phenomenon. As a superconducting spot, carrying large shielding currents, is heated up to temperatures where  $j_c$  has dropped considerably or is even zero, dissipation and a redistribution of the shielding currents will take place. We concentrate here on the second step of the instability, where more experimental information is available. Regarding the high propagation speed of the flux branches, a theoretical description of the phenomenon has to

rest on the interaction of the supercurrents with the electromagnetic field, in contrast to theories based on primarily thermal quench fronts<sup>17,18</sup>.

Our approach is similar the one used by Pippard<sup>19</sup> to study the dynamics of the quench front in bulk superconductors. We start combining Maxwell's and London's equations to the equation of motion,

$$\left(\Delta - \partial_{\alpha}^2/c^2 - 1/\lambda^2 - \mu\sigma\partial_t\right)\Phi = 0 \quad (1)$$

where  $\Delta$  is the Laplace operator,  $\partial_t$  indicates the derivative with respect to time,  $\lambda$  is the London penetration depth,  $\mu$  the magnetic permeability and  $\sigma$  the normal conductivity of the material.  $\Phi$  stands for either the electric or the magnetic field. The field equations for the normal conducting state are obtained by setting  $1/\lambda^2 = 0$ . As a simple model, we consider a straight quench front moving with the velocity  $v$ . A straightforward calculation yields the decay lengths  $l$  of the fields into the superconducting ( $l_{sc}$ ) and into the normal region ( $l_{nc}$ ). We obtain  $l_{sc} \approx \lambda$  and  $l_{nc} \approx \sqrt{Rd}$ , where  $R$  is the lateral sample dimension and  $d$  the sample thickness. Inserting typical sample dimensions yields  $l_{nc} \approx 40 \mu\text{m}$ . Thus the minimum width of any structure in the normal region must be at least  $2l_{nc} \approx 80 \mu\text{m}$  which agrees very well with the observed branch width of  $100 \mu\text{m}$ . To provide a more thorough test of our model, we determined the branch width for different samples with strongly different film thicknesses. In fig.6, we show the branch width for thin YBaCuO films (as described), NbTi sheet (thickness  $20 \mu\text{m}$ ) and sinter pellets investigated by other authors<sup>7</sup>. As one can see, the theoretical prediction represented by the straight line is in rather good agreement with the observation over several orders of magnitude in the film thickness, without any adjustable parameters involved.

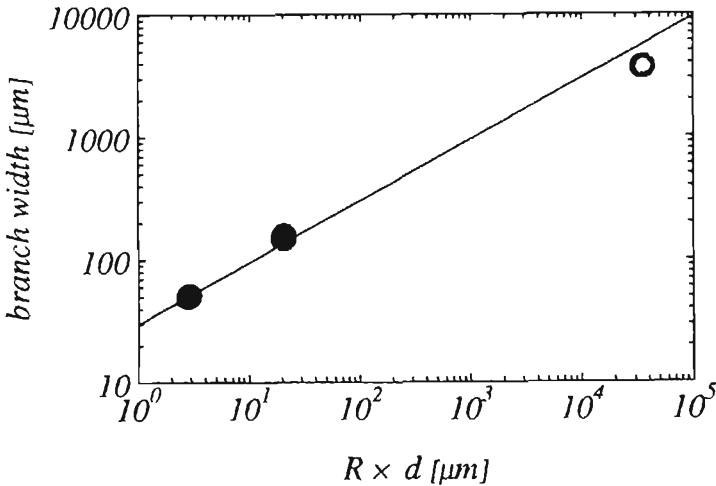


Fig.5. The branch width plotted vs the thickness of the sample. The straight line represents the theoretical model based on London's and Maxwell's equations, as described in the text. The open circle represents measurements taken from ref.7.

In order to shed light on the formation mechanism of the branches we have also carried out a linear stability analysis of a straight quench front. As the calculations show the front is stable with respect to small perturbations, as in the case of bulk superconductors<sup>20</sup>.

This suggests that the branches do not evolve from a soft mode of the straight front. In fact, it seems that the branch number grows during the whole quench process by repeated splitting of individual branches, in contrast to a soft mode mechanism which would produce a large number of evenly spaced branches from the start. Apparently, the rather uniform spacing in fig. 3c originates from the statistics of the splitting process. For a quantitative prediction of the front (or growth) velocity, detailed information about the

magnetic field distribution would be required<sup>19</sup>. In addition, eddy currents in the aluminum mirror adjacent to the superconducting film would have to be taken into account<sup>5,8</sup>.

#### 4. Conclusions

In summary, we have studied the evolution of a novel instability nucleated by a laser pulse in thin superconducting films exposed to a static magnetic field. We find two regimes, first a process where the perturbation leads to a homogeneous redistribution of flux over a certain part of the sample on a time scale less than 10ns, and a second step, where flux entering the sample from the outside penetrates the Meissner phase in the form of branches which propagate at a speed of about  $5 \times 10^4$  m/s. Some of the characteristics of this instability follow directly from a combination of Maxwell's and London's equations; others, like the origin of the branching, require further investigations. The experiments have been performed with a high- $T_C$  superconductor, but we expect similar phenomena to occur also for conventional hard type II superconductors.

We acknowledge helpful discussions with A.L.Rakhmanov and E.H.Brandt and thank P.Berberich, W.Jutzi, B.Stritzker and P.Ziemann for supplying the superconducting sample. This work was supported by Bundesministerium für Forschung und Technologie, grant 13N5705 and by the Schwerpunktprogramm Land Baden-Württemberg.

#### References

1. P.S.Swartz and C.P.Bean, *J.Appl.Phys.* **39** (1968) 4991.
2. S.L.Wipf, *Phys.Rev.* **161** (1967) 404.
3. K.Yamafuji, M.Takeo, J.Chikaba, N.Yano, F.Irie, *J.Phys.Soc.Jap.* **26** (1969) 315.
4. M.R.Freeman, *Phys. Rev. Lett.* **69** (1992) 1691.
5. R.B.Harrison, L.S.Wright, M.R.Wertheimer, *J. Appl. Phys.* **45**, (1974) 403.
6. R.B.Harrison, J.P.Pendry, L.S.Wright, *J. Low Temp. Phys.* **18** (1975) 113.
7. R.B.Harrison, L.S.Wright, M.R.Wertheimer, *Phys.Rev.* **B7** (1973) 1864.
8. M.R.Wertheimer and J.leG.Gilchrist, *J.Phys.Chem.Solids* **28** (1967) 2509.
9. R.P.Huebener and R.T.Kampwirth, *Phys.Stat.Sol. (a)* **13** (1972) 255.
10. V.Bujok, P.Brüll, J.Boneberg, S.Herminhaus, and P.Leiderer, *Appl.Phys.Lett.* **63** (1993) 412.
11. J.Fröhlingsdorf, W.Zander, and B.Stritzker, *Solid State Commun.* **67** (1988) 965.
12. P.Brüll, D.Kirchgässner, and P.Leiderer, *Physica C* **182** (1991) 339.
13. H.Theuss, A.Forkl, and H.Kronmüller, *Physica C* **190** (1992) 345.
14. D.Kirchgässner, P.Brüll, P.Leiderer, *Physica C* **195** (1992) 345.
15. P.Leiderer, J.Boneberg, P.Brüll, V.Bujok, and S.Herminhaus, *Phys.Rev.Lett.* **71** (1993) 2646.
16. T.J.Kim, J.Kowalewski, W.Assmus, and W.Grill, *Z.Phys.B-Condensed Matter* **78** (1990) 207.
17. see e.g. R.G.Mints, A.L.Rakhmanov, *Rev. of Mod. Phys.* **53** (1981) 551; R.P.Huebener, *Magnetic Flux Structures in Superconductors* (Springer-Verlag, Berlin, 1979)
18. M.I.Flik, C.L.Tien, *Transact. of the ASME, J. Heat Transfer* **112** (1990) 10.
19. A.B.Pippard, *Philos. Mag.* **41** (1950) 243.
20. H.Frahm, S.Ullah, A.T.Dorsey, *Phys. Rev. Lett.* **66** (1991) 3067.